

Transmit Power Allocation for Joint Communication and Sensing through Massive MIMO Arrays

Stefano Buzzi
DIEI

University of Cassino
and Southern Latium
Cassino, Italy
buzzi@unicas.it

Carmen D'Andrea
DIEI

University of Cassino
and Southern Latium
Cassino, Italy
carmen.dandrea@unicas.it

Marco Lops
DIETI

University "Federico II" of Naples
Naples, Italy
lops@unina.it

Abstract—The paper considers a scenario where a base station (BS), equipped with a large-scale antenna array, execute, using the same frequency range, both communication with mobile users and radar surveillance of the surrounding environment, relying on the ability of the massive MIMO array to synthesize multiple narrow beams. Based on an OFDM signaling format for both communication and surveillance tasks, a lower bound to the system achievable downlink rate is provided, along with a GLRT detection rule that does not require any knowledge about the target parameters. Then, a power allocation strategy is proposed, aimed at maximizing the fairness across the mobile users, while guaranteeing a minimum signal to interference ratio threshold value for the radar system. Numerical results show that the system performs effectively, and that the power control procedure helps in improving the system fairness.

Index Terms—massive MIMO, radar, joint communications and sensing, power allocation.

I. INTRODUCTION

Recently, there is increasing attention on the topic of the co-existence, in the same frequency band, of both radar and communication systems: see [1] for a recent review of the progress in this area. The interest in this field is justified by the progressive scaling up of frequency bands, traditionally used in radar systems, produced by the standard evolution of the cellular networks from GSM to the fifth generation (5G). Most of the work in this area has focused on the case in which the radar system and the communication system are distinct [2], [3], and has considered several degrees of cooperation, ranging from totally uncoordinated design of the two systems to the case of full cooperation. In the recent paper [4], instead, the authors have considered the case in which a base station (BS), that we nickname as radar-BS, relying on a shared large antenna array, performs both the communication and radar sensing tasks, using co-located transceivers for both functions. The paper was inspired by [5] where a similar scenario was considered with reference to a vehicular radar and communication system. The working assumption of [4] is that the massive antenna array can both operate as a MIMO radar with co-located antennas – transmitting radar signals pointing at positive elevation angles – and perform signal-space beamforming to communicate with users mainly based on the ground. It is anticipated that a radar-BS may turn out

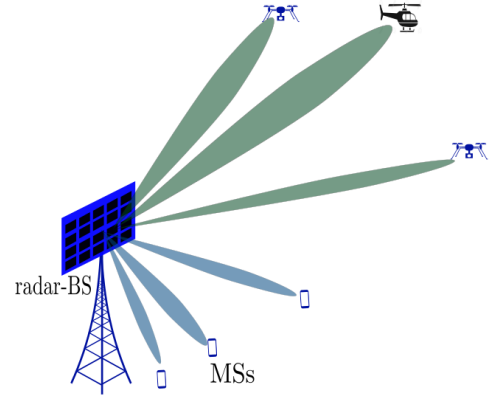


Figure 1. Representation of the considered scenario.

to be extremely popular and useful in the near future, when we expect that several unmanned flying objects will populate the sky above our heads, and it will thus be critical to be able to safely control and track them.

While in [4] the benefit of power control strategies has not been investigating, this is the main goal of this paper. Indeed, a power allocation strategy aimed at maximizing the system fairness across users of the communication system, subject to a minimum signal to interference ratio (SIR) constraint for the radar system is developed here. Our results will show that the power allocation strategy offers good performance in term of minimum rate for the users of the communication system while maintaining also good performance in term of the detection probability of the radar.

The paper is organized as follows. Next section contains the description of the considered scenario and of the channel and signal models. Section III is devoted to the description of the downlink achievable rate lower bound, while in Section IV the power allocation strategy is derived. Numerical results are discussed in Section V, while, finally, concluding remarks are given in Section VI.

II. SYSTEM MODEL

We consider the scenario depicted in Fig. 1. A radar-BS equipped with a large-scale planar antenna array with $N_A =$

$N_{A,y}N_{A,z}$ elements ($N_{A,y}$ on the horizontal axis and $N_{A,z}$ on the vertical axis), jointly serves K single-antenna mobile stations and performs surveillance tasks of the surrounding space – through electronically steered phased-array beams pointed at positive elevation angles – using the same frequency range. The time-division-duplex (TDD) protocol is used for data communication with the mobile stations, so as to exploit the uplink/downlink channel reciprocity. We denote by B the total bandwidth and by f_c the carrier frequency. Orthogonal frequency division multiplexing (OFDM) modulation is used for both communication and surveillance tasks; the total bandwidth is thus divided into M subcarriers, i.e. $B = M\Delta f$, where Δf denotes the subcarrier bandwidth.

A. Channel model

We first provide the model for the channel between the BS and the potential target. Assume that a target with radial speed v [m/sec] with respect to the radar-BS is present in the surveillance area. The channel from the BS to the target and then, upon reflection, again to the BS is modeled as a random linear time variant system with matrix-valued channel impulse response expressed as

$$\tilde{\mathbf{H}}_T(t, \tau) = \mathbf{H}_T \delta(t - \tau) e^{j2\pi\nu t}. \quad (1)$$

In (1), τ and ν denote the round-trip delay and the Doppler shift induced by the target speed; moreover, letting the pair (ϕ, θ) denote the azimuth and elevation angles of the target with respect to the BS antenna, we have $\mathbf{H}_T = \alpha_T \mathbf{a}(\phi, \theta) \mathbf{a}(\phi, \theta)^H$, with α_T a complex coefficient taking into account the target reflection coefficient and the path-loss. The vector $\mathbf{a}(\phi, \theta)$ represents the BS antenna array response vector associated with the angles (ϕ, θ) , i.e.,

$$\mathbf{a}(\phi, \theta) = \begin{bmatrix} 1, \dots, e^{-j\tilde{k}d(a_y \sin(\phi) \sin(\theta) + a_z \cos(\theta))}, \\ \dots, e^{-j\tilde{k}d((N_{A,y}-1) \sin(\phi) \sin(\theta) + (N_{A,z}-1) \cos(\theta))} \end{bmatrix} \quad (2)$$

with $\tilde{k} = 2\pi/\lambda$ the wavenumber, λ the wavelength and d the inter-element spacing.

With regard to the channel between the radar-BS and the generic k -th user, \mathbf{h}_k say, three different scenarios will be considered: Rayleigh-distributed channel, pure line-of-sight (LoS) channel with uniform phase, and Rice-distributed channels. For the Rayleigh case, we have

$$\mathbf{h}_k = \sqrt{\beta_k} \mathbf{g}_k, \quad (3)$$

where β_k subsumes the path-loss and the shadow fading coefficient, and $\mathbf{g}_k \sim \mathcal{CN}(\mathbf{0}, \mathbf{I}_{N_A})$. If the LoS channel model is in force, we have

$$\mathbf{h}_k = \sqrt{\beta_k} e^{j\psi_k} \mathbf{a}(\varphi_k, \vartheta_k), \quad (4)$$

with β_k representing the path-loss, ψ_k is the random phase uniformly distributed in $[0, 2\pi]$ and $\mathbf{a}(\varphi_k, \vartheta_k)$ is the BS antenna array response evaluated at the azimuth and elevation

angles, (φ_k, ϑ_k) say, of the k -th user. Finally, for the Rice-distributed channel we have

$$\mathbf{h}_k = \sqrt{\frac{\beta_k}{K_k + 1}} \left[\sqrt{K_k} e^{j\psi_k} \mathbf{a}(\varphi_k, \vartheta_k) + \mathbf{g}_k \right], \quad (5)$$

where the Ricean K -factor is

$$K_k = \frac{p_{\text{LoS}}(d_{k,2D})}{1 - p_{\text{LoS}}(d_{k,2D})}, \quad (6)$$

$d_{k,2D}$ is the 2D distance between the BS and the k -th user, and $p_{\text{LoS}}(d_{k,2D})$ is the LoS probability.

B. Signal model

Following [4], [5], we assume that a standard cyclic prefix (CP) OFDM modulation is used for both the communication and radar surveillance tasks, with Δf the subcarrier spacing. Let $T_0 = T_{\text{CP}} + T_s$ be the OFDM symbol duration, with T_{CP} and $T_s = 1/\Delta f$ denoting the CP and the symbol duration, respectively. The OFDM frame duration is $T_{\text{OFDM}} = NT_0$. The unit-power data symbols intended for the k -th user are denoted by $x_k(n, m)$ for $n = 0, \dots, N-1$, $m = 0, \dots, M-1$, and are arranged in a $N \times M$ grid. Similarly, the fictitious unit-power symbols used for radar detection are denoted by $x_R(n, m)$ and arranged in a $N \times M$ grid. The continuous-time OFDM signals with CP intended to the k -th user and intended for radar surveillance can be thus written as

$$s_k(t) = \sum_{n=0}^{N-1} \sum_{m=0}^{M-1} x_k(n, m) \text{rect}(t - nT_0) e^{j2\pi m \Delta f (t - T_{\text{CP}} - nT_0)}, \quad (7)$$

and

$$s_R(t) = \sum_{n=0}^{N-1} \sum_{m=0}^{M-1} x_R(n, m) \text{rect}(t - nT_0) e^{j2\pi m \Delta f (t - T_{\text{CP}} - nT_0)}, \quad (8)$$

respectively, with $\text{rect}(t)$ a rectangular pulse supported on $[0, T_0]$. Accordingly, denoting by η_k the power used by the radar-BS to transmit to the k -th user and η_R the power used for surveillance purposes on each symbol of the $N \times M$ grid, the N_A -dimensional signal transmitted by the radar-BS can be written as

$$\mathbf{s}(t) = \sum_{k=1}^K \sqrt{\eta_k} s_k(t) \mathbf{w}_k + \sqrt{\eta_R} s_R(t) \mathbf{w}_R(\phi, \theta). \quad (9)$$

In (9), \mathbf{w}_k is the beamforming vector used to transmit to the k -th user, while $\mathbf{w}_R(\phi, \theta)$ is the beamforming vector for surveillance tasks in the direction corresponding to the azimuth and elevation angles (ϕ, θ) . Two possible choices are considered in this paper for the radar beamforming vector $\mathbf{w}_R(\phi, \theta)$. The former is to use the radar-BS antenna as a phased array producing a phased beam towards the direction (ϕ, θ) , i.e.:

$$\mathbf{w}_R(\phi, \theta) = \frac{1}{\sqrt{N_A}} \mathbf{a}(\phi, \theta). \quad (10)$$

The above choice would however cause some interference to ground users; an alternative is thus to modify the beamformer in (10) in order to force to zero the interference produced

by the radar signal to the mobile users. Letting $\tilde{\mathbf{U}}$ denote a matrix whose columns form a basis for the subspace spanned by the estimated channel vectors $[\hat{\mathbf{h}}_1, \dots, \hat{\mathbf{h}}_K]$, we have thus the zero-forcing radar (ZFR) beamformer:

$$\mathbf{w}_R(\phi, \theta) = \frac{(\mathbf{I}_{N_A} - \tilde{\mathbf{U}}\tilde{\mathbf{U}}^H) \mathbf{a}(\phi, \theta)}{\|(\mathbf{I}_{N_A} - \tilde{\mathbf{U}}\tilde{\mathbf{U}}^H) \mathbf{a}(\phi, \theta)\|}. \quad (11)$$

Two comments are in order about the beamformer (11). First of all, the above equation implicitly assumes that $N_A > K$, i.e. the number of antennas at the radar-BS much be larger than the number of users in order to be able to null the beamformer projection along K signal space directions. Second, the ZFR beamformer is able to actually null to zero the interference from the radar signal to the mobile users only under the assumption of perfect channel state information; in practice, only a fraction of this interference will be canceled, depending on the accuracy of the channel estimates.

III. TRANSCEIVER PROCESSING AND DOWNLINK PERFORMANCE ANALYSIS

We now detail the transceiver processing for the channel estimation and downlink data transmission phases.

A. Uplink channel estimation

Since the BS does not transmit during this phase, the received signal will not contain any possible target echo. Let us denote by τ_c the dimension in time/frequency samples of the channel coherence length, and by $\tau_p < \tau_c$ the dimension of the uplink training phase. We also denote by $\phi_k \in \mathbb{C}^{\tau_p}$ the pilot sequence transmitted by the k -th user, with $\|\phi_k\|^2 = 1, \forall k$. Based on the above assumptions, the signal received at the radar-BS during the training phase can be therefore expressed as the following $(N_A \times \tau_p)$ -dimensional matrix:

$$\mathbf{Y}_p = \sum_{k=1}^K \sqrt{\eta_{p,k}} \mathbf{h}_k \phi_k^H + \mathbf{W}_p, \quad (14)$$

with $\eta_{p,k}$ denoting the k -th user transmitted power, and $\mathbf{W}_p \in \mathbb{C}^{N_A \times \tau_p}$ represents the thermal noise contribution and out-of-cell interference at the radar-BS. The entries of \mathbf{W}_p are modeled as i.i.d. $\mathcal{CN}(0, \sigma_w^2)$ RVs. Given the observable \mathbf{Y}_p reported in (14), the radar-BS forms the statistics $\mathbf{y}_{p,k} = \mathbf{Y}_p \phi_k$, $\forall k = 1, \dots, K$. In order to estimate the channel vectors $\mathbf{h}_k, \forall k = 1, \dots, K$, two possible channel estimation (CE) techniques will be considered: pilot matched CE (PM-CE) and linear minimum-mean-square-error CE (LMMSE-CE).

For the case of PM-CE, the channel estimate of \mathbf{h}_k is written as

$$\hat{\mathbf{h}}_k = \frac{1}{\sqrt{\eta_{p,k}}} \mathbf{y}_{p,k}. \quad (15)$$

For LMMSE-CE, instead, the channel estimate can be shown to be written as [6]

$$\hat{\mathbf{h}}_k = \mathbf{E}_k^H \mathbf{y}_{p,k}, \quad (16)$$

where

$$\mathbf{E}_k = \sqrt{\eta_{p,k}} \mathbf{R}_{y,k}^{-1} \bar{\mathbf{H}}_k, \\ \mathbf{R}_{y,k} = \sum_{i=1}^K \eta_{p,i} \bar{\mathbf{H}}_i |\phi_i^H \phi_k|^2 + \sigma_w^2 \mathbf{I}_{N_A},$$

and $\bar{\mathbf{H}}_k$ is an $(N_A \times N_A)$ -dimensional matrix depending on the adopted channel model. For the case of Rayleigh-distributed channel, Eq. (3), we have $\bar{\mathbf{H}}_k = \beta_k \mathbf{I}_{N_A}$; for the case of LoS channel, Eq. (4), we have $\bar{\mathbf{H}}_k = \beta_k \mathbf{a}(\varphi_k, \vartheta_k) \mathbf{a}^H(\varphi_k, \vartheta_k)$, while finally, for the case of Rice-distributed channel, Eq. (5), we have

$$\bar{\mathbf{H}}_k = \frac{\beta_k}{K_k + 1} [K_k \mathbf{a}(\varphi_k, \vartheta_k) \mathbf{a}^H(\varphi_k, \vartheta_k) + \mathbf{I}_{N_A}]. \quad (17)$$

B. Downlink data transmission

On the downlink, the signal received by the k -th user is expressed in discrete-time as follows:

$$y_k(n, m) = \sqrt{\eta_k} \mathbf{h}_k^H \mathbf{w}_k x_k(n, m) + \sum_{\substack{j=1 \\ j \neq k}}^K \sqrt{\eta_j} \mathbf{h}_k^H \mathbf{w}_j x_j(n, m) \\ + \sqrt{\eta_R} \mathbf{h}_k^H \mathbf{w}_R(\phi, \theta) x_R(n, m) + z_k(n, m), \quad (18)$$

where $z_k(n, m) \sim \mathcal{CN}(0, \sigma_z^2)$ is the AWGN contribution. The quantity $y_k(n, m)$ thus represents the soft estimate of the information symbol $x_k(n, m)$ and can be further processed for data detection.

Regarding the system performance analysis, starting from Eq. (18), and exploiting the use-and-then-forget bounding technique [7], the closed form achievable rate formulas, reported in Eqs. (12) and (13) at the top of next page, can be derived for the PM-CE and for the LMMSE-CE, assuming channel matched beamforming, i.e., $\mathbf{w}_k = \hat{\mathbf{h}}_k / \|\hat{\mathbf{h}}_k\|$, respectively. In these expressions, $\tau_d = \tau_c - \tau_p$ is the dimension in time/frequency samples of the downlink data transmission phase, $\gamma_k = \text{tr}(\bar{\mathbf{H}}_k)$, and $\tilde{\gamma}_k = \sqrt{\eta_{p,k}} \text{tr}(\bar{\mathbf{H}}_k \mathbf{E}_k)$. Moreover, for the case of Rayleigh channel, we have $\delta_k = \beta_k^2 N_A^2$ and $\tilde{\delta}_j^{(k)} = \beta_k^2 \text{tr}(\mathbf{E}_j^H)$; for the case of LoS channel, we have $\delta_k = 0$ and $\tilde{\delta}_j^{(k)} = 0$; and, finally, for the case of Rice channel, we have

$$\delta_k = \left(\frac{\beta_k}{K_k + 1} \right)^2 N_A (N_A + 2K_k), \quad (19)$$

$$\tilde{\delta}_j^{(k)} = \left(\frac{\beta_k}{K_k + 1} \right)^2 [\text{tr}(\mathbf{E}_j^H) + 2K_k \mathbb{R} \{ \text{tr}(\mathbf{a}^H(\varphi_k, \vartheta_k) \mathbf{E}_j^H \mathbf{a}(\varphi_k, \vartheta_k) \mathbf{E}_j) \}]. \quad (20)$$

C. Radar processing

The full derivation of the signal processing tasks for the radar is omitted for the sake of brevity. In order to perform joint radar detection in the direction defined by the angles (ϕ, θ) , given the total ignorance on the potential target reflectivity, distance and doppler frequency, upon defining the uniformly-spaced grid in the delay and Doppler domain \mathcal{G} ,

$$\mathcal{R}_k^{\text{PM}} = B \frac{\tau_d}{\tau_c} \log_2 \left(1 + \frac{\eta_k \gamma_k}{\sum_{j=1}^K \frac{\eta_j}{\eta_{p,j}} \left(\frac{\text{tr}(\mathbf{R}_{y,j} \bar{\mathbf{H}}_k)}{\gamma_j} + \eta_{p,k} \frac{\delta_k}{\gamma_j} |\phi_k^H \phi_j|^2 \right) - \eta_k \gamma_k + \eta_R \mathbf{w}_R^H(\phi, \theta) \bar{\mathbf{H}}_k \mathbf{w}_R(\phi, \theta) + \sigma_z^2} \right) \quad (12)$$

$$\mathcal{R}_k^{\text{LMMSE}} = B \frac{\tau_d}{\tau_c} \log_2 \left(1 + \frac{\eta_k \tilde{\gamma}_k}{\sum_{j=1}^K \eta_j \left(\sqrt{\eta_{p,j}} \frac{\text{tr}(\bar{\mathbf{H}}_j \mathbf{E}_j \bar{\mathbf{H}}_k)}{\tilde{\gamma}_j} + \eta_{p,k} \frac{\tilde{\delta}_j^{(k)}}{\tilde{\gamma}_j} |\phi_k^H \phi_j|^2 \right) - \eta_k \tilde{\gamma}_k + \eta_R \mathbf{w}_R^H(\phi, \theta) \bar{\mathbf{H}}_k \mathbf{w}_R(\phi, \theta) + \sigma_z^2} \right) \quad (13)$$

a Generalized Likelihood Ratio Test (GLRT) can be implemented as follows

$$\max_{\tau, \nu \in \mathcal{G}} \left| \sum_{n=0}^{N-1} \sum_{m=0}^{M-1} e^{-j2\pi\nu n T_0} e^{j2\pi m \Delta f \tau} \mathbf{u}(n, m)^H \mathbf{y}(n, m) \right|^2 \underset{H_0}{\overset{H_1}{\geq}} \gamma \quad (21)$$

In the above test, $\mathbf{y}(n, m)$ and $\mathbf{u}(n, m)$ are N_A -dimensional vectors representative of the received and transmitted signals at the radar-BS, respectively. The reader is referred to [4] for full details about the radar signal processing tasks.

IV. POWER ALLOCATION

The achievable rate lower bound for the k -th user in Eqs. (12) and (13) at the top of next page can be compactly written as

$$\mathcal{R}_k = B \frac{\tau_d}{\tau_c} \log_2 \left(1 + \frac{\eta_k \gamma_k}{\sum_{j=1}^K \eta_j \xi_{kj} + \eta_R \zeta_{k,R}(\phi, \theta) + \sigma_z^2} \right), \quad (22)$$

where $\tau_d = \tau_c - \tau_p$ is the dimension in time/frequency samples of the downlink data transmission phase. The quantities in (22), for the case of PM channel estimation, can be shown to be expressed as:

$$\gamma_k = \text{tr}(\bar{\mathbf{H}}_k), \quad \xi_{kj} = \begin{cases} \frac{1}{\eta_{p,j}} \left(\frac{\text{tr}(\mathbf{R}_{y,j} \bar{\mathbf{H}}_k)}{\gamma_j} + \eta_{p,k} \frac{\delta_k}{\gamma_j} |\phi_k^H \phi_j|^2 \right) & \text{if } j \neq k \\ \frac{1}{\eta_{p,k}} \left(\frac{\text{tr}(\mathbf{R}_{y,k} \bar{\mathbf{H}}_k)}{\gamma_k} + \eta_{p,k} \frac{\delta_k}{\gamma_k} \right) - \gamma_k & \text{if } j = k \end{cases}, \quad (23)$$

while instead, for the case of MMSE channel estimation, they are written as:

$$\gamma_k = \sqrt{\eta_{p,k}} \text{tr}(\bar{\mathbf{H}}_k \mathbf{E}_k), \quad \xi_{kj} = \begin{cases} \sqrt{\eta_{p,j}} \frac{\text{tr}(\bar{\mathbf{H}}_j \mathbf{E}_j \bar{\mathbf{H}}_k)}{\gamma_j} + \eta_{p,k} \frac{\tilde{\delta}_j^{(k)}}{\gamma_j} |\phi_k^H \phi_j|^2 & \text{if } j \neq k \\ \sqrt{\eta_{p,k}} \frac{\text{tr}(\bar{\mathbf{H}}_k \mathbf{E}_k \bar{\mathbf{H}}_k)}{\gamma_k} + \eta_{p,k} \frac{\tilde{\delta}_k^{(k)}}{\gamma_k} - \gamma_k & \text{if } j = k \end{cases}. \quad (24)$$

In the above equations, the quantities $\tilde{\delta}_j^{(k)}$, δ_j , $\mathbf{R}_{y,j}$, \mathbf{E}_j and $\bar{\mathbf{H}}_j$, depend on the adopted channel model and are reported in Section III; finally, we have $\zeta_{k,R}(\phi, \theta) = \mathbf{w}_R^H(\phi, \theta) \bar{\mathbf{H}}_k \mathbf{w}_R(\phi, \theta)$.

Given the expression of the lower bound achievable rate in Eq. (22), we formulate the following optimization problem to perform the power allocation:

$$\max_{\boldsymbol{\eta}} \min_{1, \dots, K} \mathcal{R}_k(\boldsymbol{\eta}) \quad (25a)$$

$$\text{s.t.} \quad \sum_{k=1}^K \eta_k + \eta_R \leq \frac{P_{\max}}{MN} \quad (25b)$$

$$\frac{\eta_R \|\mathbf{a}(\phi, \theta) \mathbf{a}^H(\phi, \theta) \mathbf{w}_R(\phi, \theta)\|^2}{\sum_{k=1}^K \eta_k \|\mathbf{a}(\phi, \theta) \mathbf{a}^H(\phi, \theta) \mathbf{w}_k\|^2} \geq \rho^* \quad (25c)$$

where $\boldsymbol{\eta} = [\eta_R, \eta_1, \dots, \eta_K]^T$, P_{\max} is the maximum power transmitted from the radar-BS and ρ^* is the signal-to-interference-ratio (SIR) constraint for the radar task.

Given the monotonicity of $\log_2(\cdot)$, the objective function of (25) can be equivalently rewritten as

$$\frac{\eta_k \gamma_k}{\sum_{j=1}^K \eta_j \xi_{kj} + \eta_R \zeta_{k,R}(\phi, \theta) + \sigma_z^2} \quad (26)$$

Expression (26) is quasi-concave, and so the corresponding optimization problem is quasi-concave. Problem (25) can be thus equivalently reformulated as

$$\max_{\boldsymbol{\eta}, t} \quad t \quad (27a)$$

$$\text{s.t.} \quad \frac{\eta_k \gamma_k}{\sum_{j=1}^K \eta_j \xi_{kj} + \eta_R \zeta_{k,R}(\phi, \theta) + \sigma_z^2} \geq t \quad \forall k \quad (27b)$$

$$\sum_{k=1}^K \eta_k + \eta_R \leq \frac{P_{\max}}{MN} \quad (27c)$$

$$\frac{\eta_R \|\mathbf{a}(\phi, \theta) \mathbf{a}^H(\phi, \theta) \mathbf{w}_R(\phi, \theta)\|^2}{\sum_{k=1}^K \eta_k \|\mathbf{a}(\phi, \theta) \mathbf{a}^H(\phi, \theta) \mathbf{w}_k\|^2} \geq \rho^* \quad (27d)$$

Algorithm 1 Bisection Algorithm for Solving Problem (27)

- 1: Choose the initial values of t_{\min} and t_{\max} defining a range of relevant values of the objective function in (27). Choose a tolerance $\epsilon > 0$.
- 2: **while** $t_{\max} - t_{\min} < \epsilon$ **do**
- 3: Set $t = \frac{t_{\max} + t_{\min}}{2}$
- 4: Solve the following convex feasibility program:

$$\left\{ \begin{array}{l} \frac{\eta_k \gamma_k}{\sum_{j=1}^K \eta_j \xi_{kj} + \eta_R \zeta_{k,R}(\phi, \theta) + \sigma_z^2} \geq t \quad \forall k \\ \sum_{k=1}^K \eta_k + \eta_R \leq \frac{P_{\max}}{MN} \\ \frac{\eta_R \|\mathbf{a}(\phi, \theta) \mathbf{a}^H(\phi, \theta) \mathbf{w}_R(\phi, \theta)\|^2}{\sum_{k=1}^K \eta_k \|\mathbf{a}(\phi, \theta) \mathbf{a}^H(\phi, \theta) \mathbf{w}_k\|^2} \geq \rho^* \end{array} \right. \quad (28)$$

- 5: **if** Problem (28) is feasible **then**
- 6: $t_{\min} = t$
- 7: **else**
- 8: $t_{\max} = t$
- 9: **end if**
- 10: **end while**

Table I
SIMULATION PARAMETERS

Name	Value	Description
f_c	3 GHz	carrier frequency
M	512	number of subcarriers
N	14	number of OFDM symbols
Δ_f	30 kHz	subcarrier spacing
$B = \Delta_f M$	15.36 MHz	system bandwidth
T_0	0.357 μ s	OFDM symbol duration
K	10	number of users in the cellular system
F	9 dB	noise figure at the receiver
\mathcal{N}_0	-174 dBm/Hz	power spectral density of the noise

Problem (27) can be solved efficiently by a bisection search, in each step solving a sequence of convex feasibility problems [8] as detailed in Algorithm 1.

V. NUMERICAL RESULTS

The parameters for the simulation setup are reported in Table I. We assume that the users of the communication system are randomly located on the (x, y) plane with x in $[10, 100]$ m and y in $[-50, -10] \cup [10, 50]$, with heights 1.65 m. The height of the radar-BS is 15 m. For the Rayleigh channel model in Eq. (3), we follow the three slope path loss model in [9] and we assume uncorrelated shadow fading. For the LoS channel in Eq. (4), the path-loss follows the model in [10, Table B.1.2], while for the Rice channel in Eq. (5) we use again the model in [9] and the LoS probability is evaluated following [11]. The quantity α_T in Eq. (1) containing the target reflection

coefficient and the path-loss is modeled as $\alpha_T = G \sqrt{\frac{\zeta}{L_\tau}}$, where $G = 10 \log_{10}(N_A)$ dB is the radar-BS antenna gain, $\zeta = 0.1253 \text{ m}^2$ is the target radar cross section (RCS)¹ and $L_\tau = \frac{(4\pi)^3}{\lambda^2} \left(\frac{c\tau}{2}\right)^4$. We define the Radar-Communication-Ratio (RCR) as $\text{RCR} = P_R/P_{\text{DL}}$. The scanning area of the radar system extends for $[-60, 60]^\circ$ in azimuth and for $[10, 80]^\circ$ in elevation. In the following results we compare the performance obtained with the proposed power allocation (PA) in Section IV with the uniform power allocation (Uni). In the case of Uni we assume $\eta_k = P_{\text{DL}}/(KMN)$, with $P_{\text{DL}} = 2$ W the radar-BS power budget used for communication tasks. The SIR constraint in Eq. (25c), ρ^* , is the RCR.

Fig. 2 reports the cumulative distribution functions (CDFs) of the downlink (DL) rate per user obtained in the Uni and PA cases for the three channel models discussed in Section II-A with $\text{RCR}=3$ dB, with PM-CE and MMSE-CE, and assuming the PBR approach in Eq. (10) for the radar task. Results show that performance with PA is better with respect to the one obtained in case of Uni in terms of fairness, as shown in the zoomed part of each subfigure. In particular, it is clearly seen that the PA algorithm produces a clear improvement of the lower tail of the CDF of the rates. The figure also permits assessing the impact of the CE techniques on the system performance, in particular the MMSE-CE offers better performance with respect to the PM-CE, because the former exploit the knowledge of the second order statistic of the users' channels. Fig. 3 reports the DL rate per user in the cases of Rayleigh channels for the users, fixed $\text{RCR}=3$ dB, and for two antenna configurations at the radar-BS in the case of MMSE-CE at the radar-BS using both the PBR and the ZFR in Eq. (11). The figure permits assessing the beneficial impact obtained increasing the antenna array size. Clearly, a larger antenna size permits on one hand capturing more energy when receiving, and, on the other, producing narrower beams when transmitting, which eventually results in lesser interference to the mobile stations. Additionally, we can note that the gain in performance is better in the case of PBR with respect to the one in the case of ZFR. In Fig. 4, we report the probability of detection P_D versus the target distance, using Rayleigh channel for the users and two values of RCR assuming a false alarm probability of 10^{-2} . It can be seen, as expected, that the detection performance in the case of ZFR is worse than that achieved with PBR: indeed, nulling the interference between the radar signal and the users has a negative impact on the shape of the beam used for target detection. Additionally, we can see that the performance obtained with the PA outperforms the case with Uni, so using the proposed power allocation strategy brings also some benefits in terms of detection capabilities of the system, possibly due to the radar SIR constraint present in the formulated optimization problem.

¹The RCS of a common unmanned aerial vehicle (UAV) [12] has been chosen.

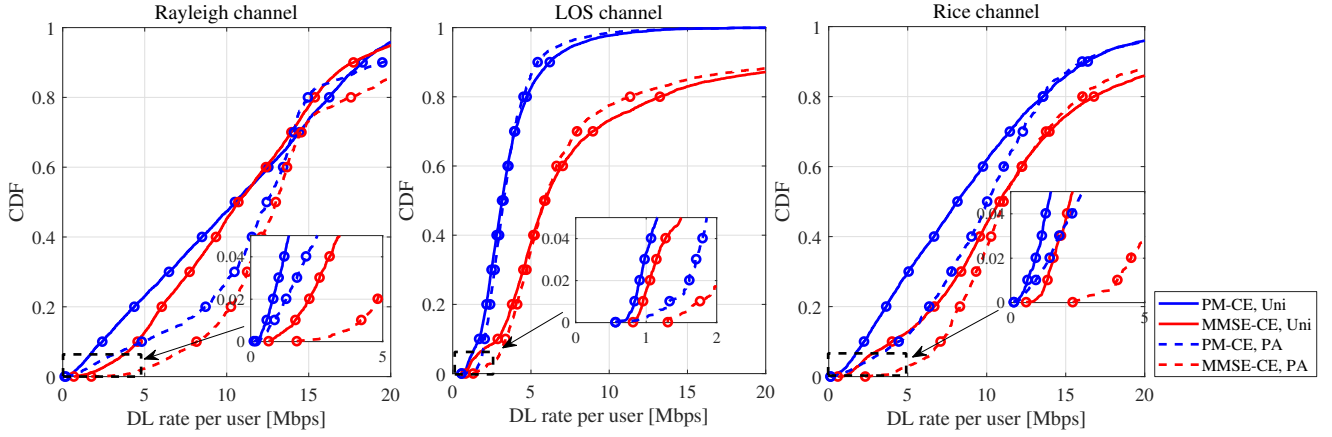


Figure 2. CDFs of DL rate per user using the PBR approach, with uniform (Uni) and proposed power allocation strategy (PA). Rayleigh channel, LoS channel and Rice channel, $\text{RCR} = 3$ dB and $N_{A,y} \times N_{A,z} = 10 \times 10$.

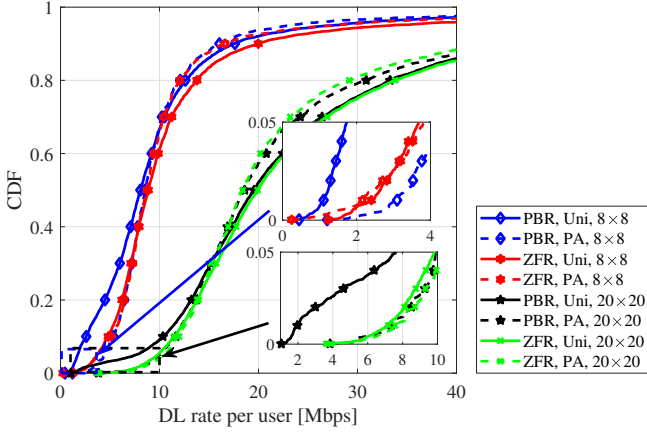


Figure 3. CDF of DL rate per user using the PBR and ZFR approaches, with uniform (Uni) and proposed power allocation strategy (PA). Rayleigh channels, $\text{RCR} = 3$ dB, two values of $N_{A,y} \times N_{A,z}$.

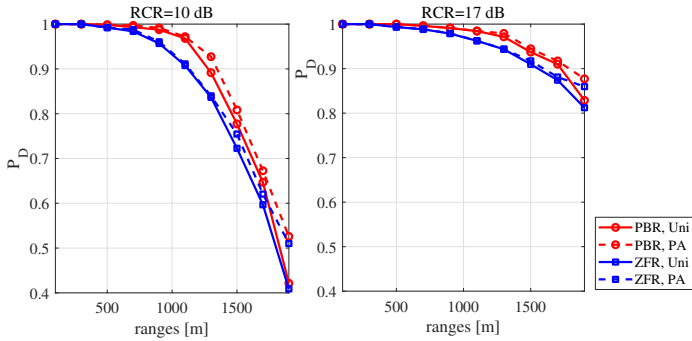


Figure 4. Probability of detection versus range using the PBR and ZFR approaches, with uniform (Uni) and proposed power allocation strategy (PA). Rayleigh channel for the users, two values of RCR , $N_{A,y} \times N_{A,z} = 10 \times 10$.

VI. CONCLUSIONS

The paper has analyzed the case in which a radar-BS equipped with massive MIMO arrays is used for joint communications and sensing tasks. Building upon the system model

and the related signal processing algorithms introduced in reference [4], a power allocation strategy that maximizes the fairness across the users on the ground with a constraint on the SIR on the radar task has been proposed and numerically assessed. Further research on this topic may be focused on the problem of devising advanced signal processing algorithms for increased performance and the capability of tracking trajectories of flying targets. This forms the object of current investigation.

REFERENCES

- [1] L. Zheng, M. Lops, Y. C. Eldar, and X. Wang, "Radar and communication coexistence: An overview: A review of recent methods," *IEEE Signal Processing Magazine*, vol. 36, no. 5, pp. 85–99, Sep. 2019.
- [2] L. Zheng, M. Lops, and X. Wang, "Adaptive Interference Removal for Un-coordinated Radar/Communication Co-existence," *IEEE Journal of Selected Topics in Signal Processing*, vol. 12, no. 1, pp. 45–60, Feb. 2018.
- [3] C. D'Andrea, S. Buzzi, and M. Lops, "Communications and radar coexistence in the massive MIMO regime: Uplink analysis," *IEEE Transactions on Wireless Communications*, vol. 19, no. 1, pp. 19–33, Jan. 2020.
- [4] S. Buzzi, C. D'Andrea, and M. Lops, "Using massive MIMO arrays for joint communication and sensing," in *2019 53rd Asilomar Conference on Signals, Systems, and Computers*, Nov. 2019, available Online <http://arxiv.org/abs/1912.00410>.
- [5] L. Gaudio, M. Kobayashi, B. Bissinger, and G. Caire, "Performance analysis of joint radar and communication using OFDM and OTFS," in *2019 IEEE International Conference on Communications Workshops (ICC Workshops)*, May 2019, pp. 1–6.
- [6] S. M. Kay, *Fundamentals of statistical signal processing*. Prentice Hall PTR, 1993.
- [7] T. L. Marzetta, E. G. Larsson, H. Yang, and H. Q. Ngo, *Fundamentals of Massive MIMO*. Cambridge University Press, 2016.
- [8] S. Boyd and L. Vandenberghe, *Convex optimization*. Cambridge university press, 2004.
- [9] S. Buzzi and C. D'Andrea, "Cell-free massive MIMO: User-centric approach," *IEEE Wireless Communications Letters*, vol. 6, no. 6, pp. 706–709, Dec. 2017.
- [10] 3GPP, "Further advancements for E-UTRA physical layer aspects (Release 9)," 3GPP TS 36.814, Tech. Rep., Mar. 2017.
- [11] 3GPP, "Study on 3D channel model for LTE," 3GPP TR 36.873 v12.0.0, Tech. Rep., Mar. 2017.
- [12] C. J. Li and H. Ling, "An investigation on the radar signatures of small consumer drones," *IEEE Antennas and Wireless Propagation Letters*, vol. 16, pp. 649–652, Jul. 2016.